A thorough explanation of the double bounded polynomial homotopy applied to non-linear circuit simulation

Une explication détaillée de l'homotopie polynômiale doublement limitée appliquée à la simulation des circuits non-linaire

Héctor Vázquez-Leal[1], Luis Hernández-Martínez[2]
Arturo Sarmiento-Reyes[2], Roberto Castañeda-Sheissa[1] and Domitilo Pereyra-Díaz[1]

***Abstract*— This work shows a new double bounded Homotopy based on polynomial formulation. It presents a bounding between two solution lines and a symmetry axis,which allows to establish a stop criterion for the simulation. Besides, the initial and final points for the new double bounded Homotopy may be established in an arbitrary manner. Mathematical properties will be introduced for this new Homotopy, besides, some mathematical and circuital examples will be discussed.**

***Résumé*— Ce travail montre une nouvelle homotopie doublement limitée, basée sur une formulation polynomiale. Il présente une limite entre deux lignes de solution, et il présente aussi un axe de symétrie; tout a permet d'établir un critère d'arrêt pour la simulation. D'ailleurs, les points initial et final pour la nouvelle homotopie doublement limitée, peuvent être établie de manière arbitraire. Les propriétés mathématiques seront mises en place pour cette nouvelle homotopie, et en plus, quelques exemples mathématiques et exemples de circuits seront discutés.**

***Index Terms*— Homotopy continuation methods, DC analysis, path following techniques.**

I. Introduction

The research and development in the electronics industry has proven being very important activities on developed countries, causing a big impact in their economies, creating better conditions for development of their population and offering conditions to improve their performance on daily duties. The electronics industry, as demanding as competitive, constantly is pushing the physical area of circuits to the very limits of human knowledge. As a consequence, the rapid growth of integration levels for integrated circuits (IC). In fact, the 2 billion transistor mark was reached in 2008. Also, the noticeable advance in technologies at nanometer scales has affected other knowledge areas like device modeling, simulation techniques for integrated circuits, materials science, among others. Therefore, it is necessary to develop new and better simulation techniques for the purpose of simulate the behavior of circuits that have become more complex. Specifically, the Homotopy has a direct impact in IC simulation tools and, in general, in whichever science area where the phenomenon can be modeled by non-linear equations system.

Integrated circuits could have more than one operating point or DC solution, one way to resolve such points is by the use of Homotopy methods [1]. The problem to find solutions in DC is important because this analysis serves as initial point for the rest of analysis performed routinely during the circuit design (for instance, small signal analysis)[6]. This analysis consists in finding solutions for non-linear algebraic equations system (NAEs) originating from integrated circuits [9]. These NAEs become complex because the accelerated increase on the number of transistors by ICs and the increase of complexity of models (as the result of reducing the physical dimensions of the components) causing two situations: existence for multiple unexpected operating points, and lack

H. Vázquez, R. Castañeda and D. Pereyra are with the Universidad Veracruza, Facultad de Instrumentación Electrónica y Ciencias Atmosféricas, Xalapa, Veracruz, Mexico. E-mail: [hvazquez]@uv.mx

L. Hernández , A. Sarmiento are with the Electronics Department, CAD Group, National Institute for Astrophysics Optics and Electronics (INAOE), P.O. Box 51, 72000, Puebla, Pue., Mexico. E-mail: [luish, jarocho]@inaoep.mx

of convergence to the operating point in Newton's method.

The Newton-Raphson method (NR) is employed in many circuit simulators for integrated circuit. The widespread use of the NR method is its quadratic convergence rate [6], [2] which minimizes computation times in simulations. Nevertheless, the NR method has certain convergence problems [2], [9] like: oscillation and divergence. Convergence problem becomes apparent in electronics when non-linear equation systems ($f(x)$) from elaborated systems are resolved, and these complicated systems mix analog and digital blocks. Therefore, the need to develop backup methods or replace the NR method.

Electronic circuit designers usually deal with convergence failures using the NR method, thus as last resource, some parameters in the numerical engine of the simulator are modified hoping to reach convergence. This situation breaks design schedules. Also, justifies the use of alternate methods to NR like Homotopy to locate the operating point. Nevertheless, there are many reasons for using Homotopy like occurrence of more than one operating point. That is, unlike the NR method, Homotopy is capable to locate multiple operating points. This is very important because it may occur that a designer provides one operating point as valid in DC (found by the NR method) but other operating point, one of many that the circuit may contain, is physically present in the already fabricated circuit. This may translate into the circuit malfunctioning with costly consequences for a company.

This situation has prompted investigations to develop new methods capable to solve non-linear equation systems in an efficient and accurate process.

Homotopy methods [7], [14], [3], [17], [5] are valuable tools for simulation, presented as an alternate method to the NR method. However, Homotopy methods have two problems: stop criterion and computing time.

II. Double Bounded Homotopy

Considering the existence of two solution lines [16], [15], one at $\lambda = a$ and the other at $\lambda = b$; so the Homotopy formulation is:

$$\boldsymbol{H}(\boldsymbol{f}(\boldsymbol{x}), \lambda) = \mathbf{0} \tag{1}$$

where $f(x)$ is the equilibrium equation, λ is the Homotopy variable, and $\boldsymbol{H}^{-1}(\mathbf{0})$ are the family of solutions that outlines the Homotopy patch, such that:

- For $\lambda = 0.5(a+b)$ solution for $H^{-1}(0)$ is known or simple to calculate computationally. This point is known as initial point in Homotopy (λ_i).
- For $\lambda = a$, $\boldsymbol{H}(\boldsymbol{f}(\boldsymbol{x}), \boldsymbol{a}) = \boldsymbol{f}(\boldsymbol{x})$. It means that at $\lambda = a$ all solutions for $\boldsymbol{f}(\boldsymbol{x})$ are located.
- For $\lambda = b$, $\boldsymbol{H}(\boldsymbol{f}(\boldsymbol{x}), \boldsymbol{b}) = \boldsymbol{f}(\boldsymbol{x})$. Means that at $\lambda = b$ all solutions for $\boldsymbol{f}(\boldsymbol{x})$ are located.
- The path for $\boldsymbol{H}^{-1}(\mathbf{0})$ is a continuous function for λ in the range of $a \leq \lambda \leq b$.

III. Double Bounded Polynomial Homotopy

The double bounded polynomial Homotopy (DBP) is defined by the following equation:

$$\boldsymbol{H}(\boldsymbol{f}(\boldsymbol{x}), \lambda) = Q(x - x_i)(x - x_f) - C(\lambda - a/2)^2 \boldsymbol{f}(\boldsymbol{x})^2 \tag{2}$$

where $Q = \lambda(\lambda - a)$, a is a constant that represents the separation between solution lines, x_i is the initial point, x_f the final point, and C an arbitrary constant.

Based on the preceding, Homotopy can be expressed in general way as:

$$\boldsymbol{H}(\boldsymbol{f}(\boldsymbol{x}), \lambda) = \begin{cases} f(x^*) = 0 & \text{para } \lambda = 0 \text{ y } x = x^* \\ (x - x_i)(x - x_f) = 0 & \text{para } \lambda = a/2 \\ f(x^*) = 0 & \text{para } \lambda = a \text{ y } x = x^* \end{cases}$$

where x^* is any solution for the equilibrium equation $f(x)$, x_i in the initial point, while x_f is the final point for outline the path.

This Homotopy has two solution lines ($\lambda = 0$ y $\lambda = a$). Squaring function $f(x)$ originates an even number of solutions (or operating points) resulting in the bounding of it and closes the Homotopy path within the middle region. Figure 1 shows how the Homotopy path initiates at $A = (x_i, a/2)$ on the symmetry axis, finds two roots (in region $\lambda_2(x)$) and, finally, ends when a new crossing the symmetry axis at $B = (x_f, a/2)$ meaning that the tracing of a symmetrical branch is completed fulfilling the stop criterion.

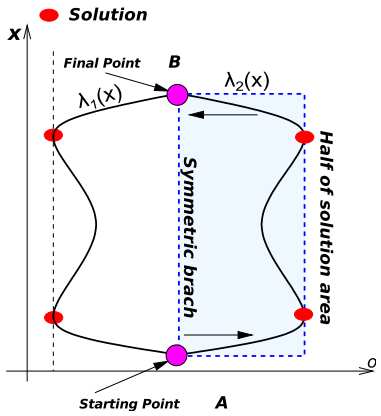

Fig. 1: Stop criterion.

Properties of this new Homotopy are presented in the following sub-sections:

A. Symmetrical branches

Symmetrical branches shown in figure 1 can be obtained solving for λ equation 2. The result is two symmetrical branches (ecuaciones 3 y 4), where each symmetrical branch $\lambda_1(x)$ and $\lambda_2(x)$is tied to a different solution line $\lambda = 0$ and $\lambda = a$, respectively. Given that $\lambda_1(x)$ and $\lambda_2(x)$ are connected and symmetrical, it is just necessary to trace only one of them to obtain the complete path and finish the simulation. $\lambda_2(x)$ is chosen as the path to trace, it touches tangentially solution line $\lambda = a$.

$$\lambda_1(x) = \frac{\left(\sqrt{1 - \frac{C(f(x))^2}{(x-x_i)(x-x_f)}} - 1\right) a}{2\sqrt{1 - \frac{C(f(x))^2}{(x-x_i)(x-x_f)}}} \tag{3}$$

$$\lambda_2(x) = \frac{\left(\sqrt{1 - \frac{C(f(x))^2}{(x-x_i)(x-x_f)}} + 1\right) a}{2\sqrt{1 - \frac{C(f(x))^2}{(x-x_i)(x-x_f)}}} \tag{4}$$

To demonstrate that $\lambda_1(x)$ is linked to the solution line $\lambda = 0$, the following limit is calculated:

$$\lim_{f(x)\to 0} \lambda_1(x) = 0 \tag{5}$$

the equilibrium equation $f(x)$ tends to zero when x tends to solution x^*, as shown in the following limit calculation:

$$\lim_{x\to x^*} f(x) = 0 \tag{6}$$

Now, to demonstrate that $\lambda_2(x)$ is linked to the solution line $\lambda = a$, the following limit is calculated:

$$\lim_{f(x)\to 0} \lambda_2(x) = a \tag{7}$$

B. Symmetry axis

Symmetry axis is an important property in the double bounded Homotopy. In the particular case of the double bounded polynomial Homotopy the symmetry axis is:

$$\lambda_{sym} = \frac{a}{2} \tag{8}$$

This symmetry axis belongs to the symmetry relationship between $\lambda_1(x)$ and $\lambda_2(x)$.

As shown in figure 2, the following relationship must be satisfied:

$$\lambda_2(x) - \lambda_{sym} = \lambda_{sym} - \lambda_1(x)$$

Replacing the value for λ_{sym} it is obtained that:

$$\lambda_2(x) - 0.5a = 0.5a - \lambda_1(x)$$

Reordering terms:

$$\lambda_2(x) + \lambda_1(x) = a$$

Substituting values for $\lambda_1(x)$ and $\lambda_2(x)$ by their respective functions, the following relationship is obtained:

$$a = a$$

Removing terms results:

$$0 = 0$$

Proofing this equality shows that the Homotopy path is symmetrical around the symmetry axis.

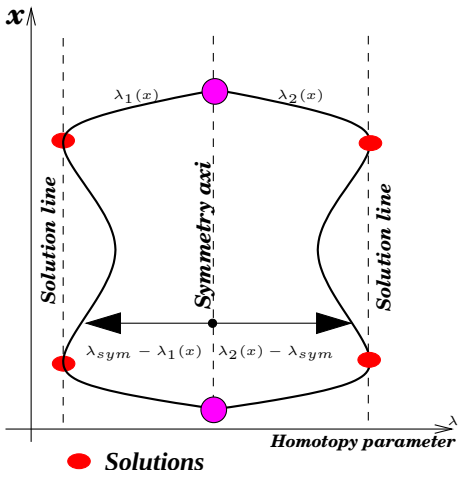

Fig. 2: The homotopy path have symmetry

C. Initial point and final point

The point where the Homotopy path starts lays right on the symmetry axis, meaning that $\lambda_i = 0.5a$. Therefore, replacing λ_i in equation 2 the term that contains the equilibrium equation $f(x)$ is canceled, resulting:

$$\boldsymbol{H}(\boldsymbol{f}(\boldsymbol{x}), \lambda_i) = (x - x_i)(x - x_f) = 0$$

So the initial (x_i) and final (x_f) points are chosen arbitrarily.

In order to prove that $\lambda_1(x)$ crosses the symmetry axis at x_i and x_f, the following limits are calculated:

$$\begin{aligned} \lim_{x\to x_i} \lambda_1(x) &= 0.5a \\ \lim_{x\to x_f} \lambda_1(x) &= 0.5a \end{aligned} \tag{9}$$

To demonstrate that $\lambda_2(x)$ crosses the symmetry axis at x_i and x_f, the following limits are calculated:

$$\begin{aligned}\lim_{x\to x_i}\lambda_2(x) &= 0.5a\\ \lim_{x\to x_f}\lambda_2(x) &= 0.5a\end{aligned} \tag{10}$$

Therefore, when x tends to the value of initial point x_i or final point x_f, the Homotopy parameter λ tends to the symmetry axis at $\lambda = 0.5a$.

D. Circuital rendering

Circuital rendering for the double bounded Homotopy can be derived solving $f(x)$ from the Homotopy expression in equation 2. From former equation can be deduced that non-linear current sources are present (K_1, ... ,K_n) connected to every node of the circuit, where n is the number of nodes and l the number of constant voltage sources (E).

$$I_{K_m} = \frac{\lambda(\lambda-a)(V_m - V_i)(V_m - V_f)}{(\lambda - a/2)^2} \tag{11}$$

where $m = [1, n]$, V_{xk} are nodal voltages for the circuit, V_{xk_i} and V_{xk_f} are constants related to initial and final points for each variable V_{xk} of the Homotopy. Again, from equation (2), it can be deduced that non-linear voltage sources are present (K_n, ... ,K_{n+1}) connected to every node of the circuit, where n is the number of nodes and l the number of constant voltage sources (E).

$$V_{K_{n+m}} = \frac{\lambda(\lambda-a)(I_m - I_i)(I_m - I_f)}{(\lambda - a/2)^2} \tag{12}$$

where $m = [1, l]$, V_{xk} are nodal voltages for the circuit, V_{xk_i} and V_{xk_f} are constants related to initial and final points for each variable V_{xk} of the Homotopy.

Finally, circuital rendering of the Homotopy at the symmetry axis can be seen in figure 3.

E. Multiple variables

When the Homotopy is applied to a non-linear equation system with multiple variables, generalization is given by:

$$\begin{aligned}
H_1(f_1(x),\lambda) &= \lambda(\lambda-a)(x_1-x_i)(x_1-x_f) - C(\lambda-a/2)^2 f_1(x)^2\\
H_2(f_2(x),\lambda) &= \lambda(\lambda-a)(x_2-x_i)(x_2-x_f) - C(\lambda-a/2)^2 f_2(x)^2\\
H_3(f_3(x),\lambda) &= \lambda(\lambda-a)(x_3-x_i)(x_3-x_f) - C(\lambda-a/2)^2 f_3(x)^2\\
&\vdots \qquad\qquad \vdots \qquad\qquad \vdots\\
H_n(f_n(x),\lambda) &= \lambda(\lambda-a)(x_n-x_i)(x_n-x_f) - C(\lambda-a/2)^2 f_n(x)^2
\end{aligned}$$

where n is the number of equations for the equilibrium equation $\boldsymbol{f}(\boldsymbol{x})$, f_i represents every nodal equations or equations for the non-NA compatible elements [8] and C is an arbitrary constant.

There are n^2 points, in total, where the path could start, resulting from the combinatorial of initial and final points from each variable x. In fact, an initial point may become the final point if the path starts right on the other side of the Homotopy path.

F. Curvature radius

The curvature radius for the Homotopy path is used as means to analyze (*qualitatively*) the behavior of paths at strategic points like solutions and turning points (see figure 4). The curvature radius for a curve at a given point is the radius of a circle with the curvature equivalent at that point on the curve. The equation for the curvature radius is:

$$\rho = \left| \frac{(1 + (y')^2)^{3/2}}{y''} \right|$$

where y is a function $y(x)$, y' is the first derivative of $y(x)$ with respect to x and y'' is the second derivative of $y(x)$ with respect to x. In terms of the Homotopy path, the first derivative y' equals to $\frac{d\lambda}{dx}$ and the second derivative y'' equals to $\frac{d^2\lambda}{dx^2}$.

The slope for the Homotopy path at solution and turning points is zero ($y' = \frac{d\lambda}{dx} = 0$), this property can be used to simplify the expression for the curvature radius at those points, as follows:

$$\rho = \left| \frac{1}{\frac{d^2\lambda}{dx^2}} \right|$$

Now, λ_2 is derived twice with respect to x from equation 4, considering a and C as constants. After derivation $f(x)$ is superseded by zero because is the solution point, giving as result:

$$\rho_s = \left[2\,\frac{(x-x_i)\,(x-x_f)}{aC\left(\frac{d}{dx}f\,(x)\right)^2} \right]_{x=x_s}$$

here x_s is the solution point, C is an arbitrary constant of the Homotopy, and a represents the separation between solution lines.

Equation ρ_s allows to conclude that distance a between solution lines affects the acute of the Homotopy path at solutions, in such a way that the curve becomes more sharp as solution lines separates (from each other) and flattens as solution lines unite. Besides, constant C is inversely proportional to the curvature radius.

The point where the path returns to the search of solutions is called turning point ρ_r. The study of the curvature radius is completed with the study

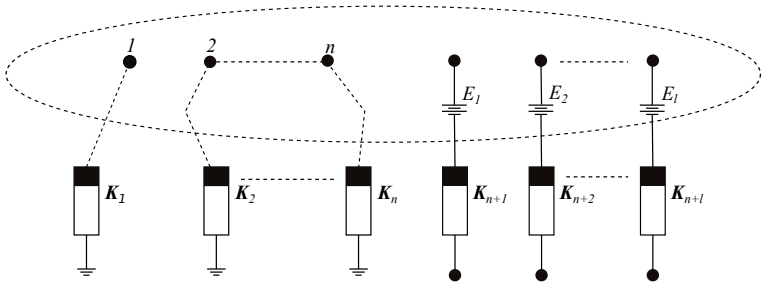

Fig. 3: Circuital rendering for the double bounded Homotopy.

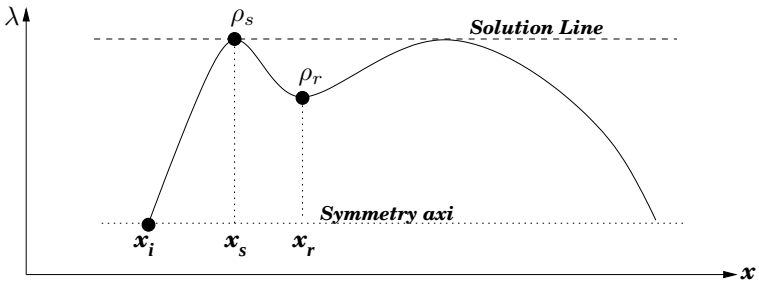

Fig. 4: Solution point ρ_s and turning point ρ_r

of the curvature at solutions ρ_s in order to understand in more detail the qualitative behavior of the Homotopy path. At the turning point the derivative of λ with respect to x equals zero. Besides, the turning point spatially matches with the critical points of function $f(x)$, so the derivative for $f(x)$ with respect to x is zero. Hence, the equation for the curvature radius is subdivided into the terms shown in Table I:

The curvature radius is:

$$\rho_r = \frac{1}{(r_1 + r_2 + r_3 + r_4)}$$

Assuming that the second derivative of $f(x)$ with respect to x evaluated at x_r is real and different to zero; the next step is to qualitatively evaluate the behavior of the curvature radius with the following limits:

$$\lim_{f(x_r)\to+\infty} |\rho_r| = \infty \tag{13}$$

$$\lim_{f(x_r)\to+0} |\rho_r| = \infty \tag{14}$$

$$\lim_{a\to+\infty} |\rho_r| = 0 \tag{15}$$

$$\lim_{a\to+0} |\rho_r| = \infty \tag{16}$$

The limit for equations 13 and 14 imply that when $f(x)$ tends to big o very small values, curvature radius grows, so the curve will be flat. As for the case when $f(x)$ has big values (evaluated at turning point x_r) is fairly common on the nodal equations of the circuit. Hence, the Homotopy path will tend to remain (flat) close to solution line $\lambda = a$. Since C is being multiplied by $f(x)$, small values for C can be employed in order to reduce the curvature radius. On the other hand, the limits for equations 15 and 16 shows that the curvature radius is inversely proportional to the separation value between solution lines a. The former suggests that values for a and C can be combined to reduce the proximity of the Homotopy path to the solution line. Finally, all the results for the curvature radius may be extrapolated to the solution line $\lambda = 0$ because the symmetry of the paths.

IV. Study cases

This section will show Homotopy simulations for mathematical and circuital cases in order to expose the new proposed method to a variety of non-linear functions.

A. Mathematical case

To illustrate the use of Homotopy in a bi-dimensional example, the Homotopy is applied to the following NAEs:

$$f_1(x_1, x_2) = (x_2 - 1)(x_2 - 4)(x_2 - 6) + x_1 = 0$$
$$f_2(x_1, x_2) = (x_1 - 3)(x_1 - 6)(x_1 - 9) + x_2 = 0$$

where x_1 and x_2 are variables for the equation system.

Graphical solution of the system is shown in figure 5a.

The proposed Homotopy formulation is:

Component
$r_1 = \left[\frac{\left(\frac{C(f(x))^2}{(x-x_i)^2(x-x_f)} + \frac{C(f(x))^2}{(x-x_i)(x-x_f)^2} \right)^2 a}{\left(1 - \frac{C(f(x))^2}{(x-x_i)(x-x_f)}\right)^2} \right]_{x=x_r}$
$r_2 = \left[1/4 \frac{\left(-2\frac{Cf(x)\frac{d^2f(x)}{dx^2}}{(x-x_i)(x-x_f)} - 2\frac{C(f(x))^2}{(x-x_i)^3(x-x_f)} - 2\frac{C(f(x))^2}{(x-x_i)^2(x-x_f)^2} - 2\frac{C(f(x))^2}{(x-x_i)(x-x_f)^3} \right) a}{\left(1 - \frac{C(f(x))^2}{(x-x_i)(x-x_f)}\right)} \right]_{x=x_r}$
$r_3 = \left[3/8 \frac{\left(\sqrt{1 - \frac{C(f(x))^2}{(x-x_i)(x-x_f)}} + 1 \right) a \left(\frac{C(f(x))^2}{(x-x_i)^2(x-x_f)} + \frac{C(f(x))^2}{(x-x_i)(x-x_f)^2} \right)^2}{\left(1 - \frac{C(f(x))^2}{(x-x_i)(x-x_f)}\right)^{5/2}} \right]_{x=x_r}$
$r_4 = \left[\frac{2\left(\sqrt{1 - \frac{C(f(x))^2}{(x-x_i)(x-x_f)}} + 1 \right) a \left(\frac{Cf(x)\frac{d^2f(x)}{dx^2}}{(x-x_i)(x-x_f)} + \frac{C(f(x))^2}{(x-x_i)^3(x-x_f)} + \frac{C(f(x))^2}{(x-x_i)^2(x-x_f)^2} + \frac{C(f(x))^2}{(x-x_i)(x-x_f)^3} \right)}{4\left(1 - \frac{C(f(x))^2}{(x-x_i)(x-x_f)}\right)^{3/2}} \right]_{x=x_r}$

TABLE I: Curvature radius terms of ρ_r

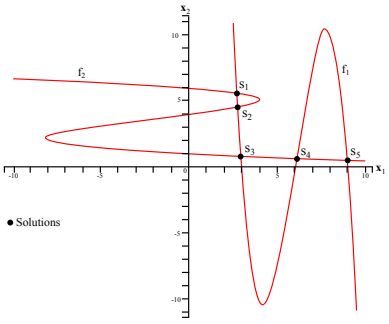

(a) Five solution system

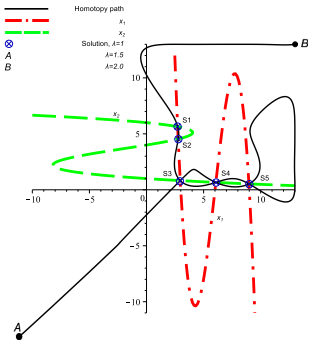

(b) Homotopy path for a two variable example

Fig. 5: Mathematical case.

$$H_1(f_1, \lambda) = \lambda(\lambda - 1)(x_1 - 13)(x_1 + 13) - (\lambda - 0.5)^2 f_1^2 = 0$$
$$H_2(f_2, \lambda) = \lambda(\lambda - 1)(x_2 - 13)(x_2 + 13) - (\lambda - 0.5)^2 f_2^2 = 0$$

here the solution system is located at $\lambda = 0$ and at $\lambda = 1$. For practical purposes just one symmetrical branch is employed to trace the Homotopy path, this branch is linked to solution line $\lambda = 1$.

As starting point it was chosen $A = (x_1 = -13, x_2 = -13)$ and path tracing starts, the result is a global convergence for all solutions of the system (S_1, S_2, S_3, S_4 y S_5) (see figure 5b). The final point is $B = (x_1 = 13, x_2 = 13)$ and the Homotopy path for variables x_1 and x_2 is shown in figures 6a and 6b, respectively.

B. *Circuit with two tunnel diodes*

Tunnel diodes have non-linear behavior, which can be described in a general way in figure 7a. As it can be seen in this figure, tunnel diode has 3 sign changes for the slope and combined with a load line could produce up to 3 solutions for a tunnel diode present in the circuit. The model chosen for the tunnel diode in this example is a function of exponential terms [11],[10] and can be expressed as:

$$i = I_p(\frac{V}{V_p})e^{1-\frac{V}{V_p}} + I_0 e^{\frac{q}{KT}V}$$

This example presents a circuit (ERDD) with 2 tunnel diodes, one voltage source and one resistor, all of them are in series (see figure 7b). The voltage source V_1 is at $1V$ and the value for the resistor R_2 is 20Ω. Besides, both tunnel diodes (K_3 and K_4) have the same model with coefficients:

$Ip = 100 \times 10^{-3}$, $V_p = 50 \times 10^{-3}$, $I_0 = 1 \times 10^{-9}$, and $\frac{q}{KT} = 40$. The equilibrium equation is formulated based on the modified nodal analysis (MNA) of the circuit. Also, the system is reduced to 3 equations discarding the nodal voltage v_1 because is constant and equals to the voltage source. Therefore, the variables for the resulting system are: I_E, v_2, and v_3. Equations are expressed as follows:

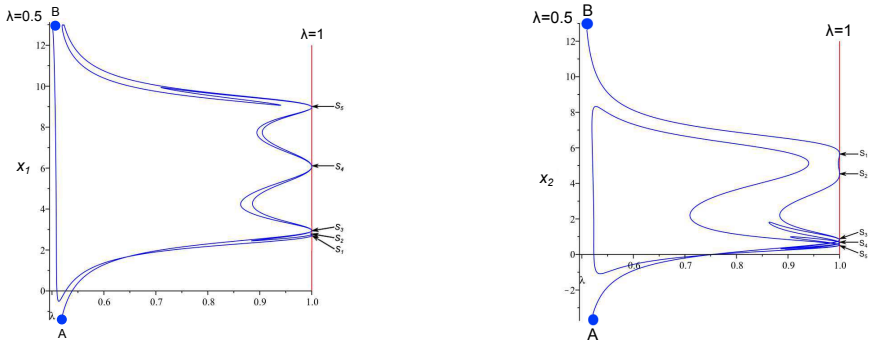

(a) Homotopy path $\lambda - x_1$

(b) Homotopy path $\lambda - x_2$

Fig. 6: Homotopic paths.

$$
\begin{aligned}
f_1 &= \tfrac{1}{20} - \tfrac{v_2}{20} + I_E = 0 \\
f_2 &= -\tfrac{1}{20} + \tfrac{v_2}{20} + 2(v_2 - v_3)e^{(1-20v_2+20v_3)} \\
&+1 \times 10^{-9} e^{(40v_2-40v_3)} = 0 \\
f_3 &= 2(v_2 - v_3)e^{(1-20v_2+20v_3)} + 1 \times 10^{-9} e^{(40v_2-40v_3)} \\
&-2v_3 e^{(1-20v_3)} - 1 \times 10^{-9} e^{(40v_3)} = 0
\end{aligned}
\tag{17}
$$

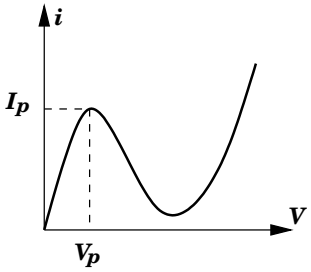

(a) Tunnel diode model

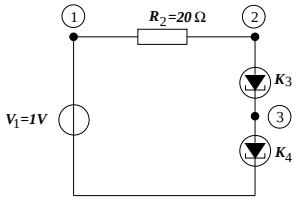

(b) Circuit with two tunnel diodes

Fig. 7: Example with tunnel diodes.

Now, the DBH is applied to solve the circuit. The Homotopy formulation is given as:

$$
\begin{aligned}
H_1(f_1, \lambda) &= \lambda(\lambda - 1)(I_E - 1)(I_E + 1) - (\lambda - 0.5)^2 f_1^2 = 0 \\
H_2(f_2, \lambda) &= \lambda(\lambda - 1)(v_2 - 1)(v_2 + 1) - (\lambda - 0.5)^2 f_2^2 = 0 \\
H_3(f_3, \lambda) &= \lambda(\lambda - 1)(v_3 - 1)(v_3 + 1) - (\lambda - 0.5)^2 f_3^2 = 0
\end{aligned}
$$

where the bounding lines are $a = 0$ and $b = 1$, and the initial point for the Homotopy path is selected as $A = [I_E = -1, v_2 = -1, v_3 = -1, \lambda = 0.5]$.

As result of the tracing for the the Homotopy path, all the operating points of the circuit are located, nine in total (Figure 8(a)). In order to make the results clearer, Homotopy path and the equilibrium equation are presented as function of the branch voltages ($u_2 = v_2 - v_3$ y $u_3 = v_3$) of the tunnel diodes. This depiction allows to trace the homotopy path in terms of the branch functions of the tunnel diodes. Figure 8(a) shows the complete symmetric path associated to the bounding line $\lambda = 1$ against branch current u_2. Besides, the final point for the path was located at $B = [I_E = 1, v_2 = 1, v_3 = 1, \lambda = 0.5]$. Figure 8(b) shows a close-up to the solutions region, here can be seen how the path crosses through all 9 solutions, this presents 3 regions ($F1$, $F2$ y $F3$) of close roots. To observe in detail the behavior of the path, a close-up for every one of regions $F1$, $F2$, and $F3$ is performed, these are shown in figures 8(c), 8(d), and 8(e)), respectively. In those figures all solutions are shown found by the Homotopy path.

C. Circuit with bipolar transistors and a diode

A circuit with bipolar transistors and a diode was reported by [12] and [18], it was originally solved using piecewise methods. Then, in [19], the circuit was solved by fixed point modified Homotopy. This circuit has 3 operating points. All transistors are modeled using Ebers-Moll. The equation of this model is:

$$
\begin{bmatrix} i_{D_E} \\ i_{D_C} \end{bmatrix} = \begin{bmatrix} 1 & \alpha_R \\ \alpha_F & 1 \end{bmatrix} \begin{bmatrix} 10^{-9}(e^{(40v_{be})} - 1) \\ 10^{-9}(e^{(40v_{bc})} - 1) \end{bmatrix}
$$

The circuital depiction of the model is shown in figure 10.

The model for the diode is:

$$
i_d = 10^{-9}(e^{40u} - 1)
$$

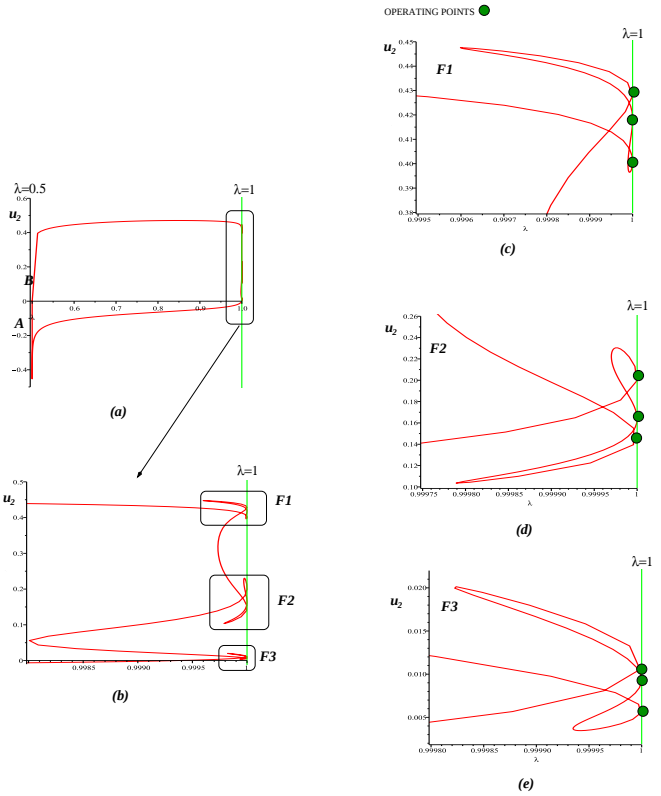

Fig. 8: Homotopy path (u_2-λ) for the circuit with tunnel diodes.

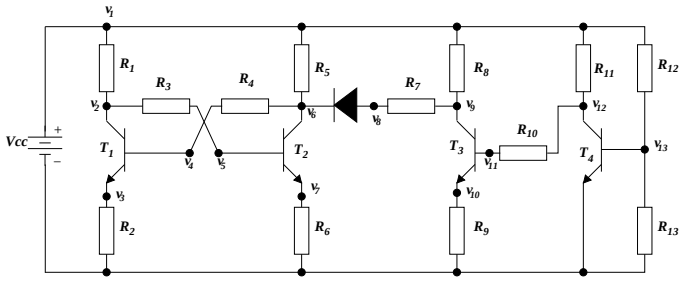

Fig. 9: Circuit with bipolar transistors and a diode.

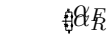

Fig. 10: Ebers-Moll model for the bipolar transistor.

The values for the components in the circuit can be found in table II. First, equilibrium equation is formulated using the modified nodal analysis resulting in a system with 14 equations and 14 variables. The circuit is shown in figure 9 and its nodal equations (Equilibrium Equations) are shown on table III (using MNA analysis).

Now, the DBH is applied to solve the circuit. The Homotopy formulation is expressed as follows:

$$
\begin{aligned}
H_1(f_1,\lambda) &= \lambda(\lambda-1)(v_1-13)(v_1+13) - C(\lambda-0.5)^2 f_1^2 = 0\\
H_2(f_2,\lambda) &= \lambda(\lambda-1)(v_2-13)(v_2+13) - C(\lambda-0.5)^2 f_2^2 = 0\\
&\vdots\\
H_{14}(f_{14},\lambda) &= \lambda(\lambda-1)(I_E-13)(I_E+13) - C(\lambda-0.5)^2 f_{14}^2 = 0
\end{aligned}
$$

Component	Value
R_1	$4K\Omega$
R_2	$0.1K\Omega$
R_3	$8K\Omega$
R_4	$8K\Omega$
R_5	$4K\Omega$
R_6	$0.1K\Omega$
R_7	$30K\Omega$
R_8	$1K\Omega$
R_9	$0.1K\Omega$
R_{10}	$10K\Omega$
R_{11}	$4K\Omega$
R_{12}	$10K\Omega$
R_{13}	$1K\Omega$
V_{cc}	$12V$

TABLE II: Circuit components.

where the constant value C is $C = 0.1$, bounding lines are $a = 0$ and $b = 1$, and the initial point of the Homotopy path is selected as shown in table IV.

f_1	$\frac{37}{20000}\,v_1 - \frac{1}{4000}\,v_2 - \frac{1}{4000}\,v_6 - \frac{1}{1000}\,v_9 - \frac{1}{4000}\,v_{12} - \frac{1}{10000}\,v_{13} + IE = 0$
f_2	$-\frac{1}{4000}\,v_1 + \frac{3}{8000}\,v_2 - \frac{1}{8000}\,v_5 + 0.00000000990\,e^{40\,v_4 - 40\,v_3} + 0.00000000010 - 0.000000010\,e^{40\,v_4 - 40\,v_2} = 0$
f_3	$\frac{1}{100}\,v_3 - 0.000000010\,e^{40\,v_4 - 40\,v_3} + 0.00000000990 + 0.00000000010\,e^{40\,v_4 - 40\,v_2} = 0$
f_4	$\frac{1}{8000}\,v_4 - \frac{1}{8000}\,v_6 + 0.00000000010\,e^{40\,v_4 - 40\,v_3} - 0.00000001000 + 0.00000000990\,e^{40\,v_4 - 40\,v_2} = 0$
f_5	$-\frac{1}{8000}\,v_2 + \frac{1}{8000}\,v_5 + 0.00000000010\,e^{40\,v_5 - 40\,v_7} - 0.00000001000 + 0.00000000990\,e^{40\,v_5 - 40\,v_6} = 0$
f_6	$-\frac{1}{4000}\,v_1 - \frac{1}{8000}\,v_4 + \frac{3}{8000}\,v_6 + 0.00000000990\,e^{40\,v_5 - 40\,v_7} + 0.00000001010 - 0.000000010\,e^{40\,v_5 - 40\,v_6} - 0.000000010\,e^{40\,v_8 - 40\,v_6} = 0$
f_7	$\frac{1}{100}\,v_7 - 0.000000010\,e^{40\,v_5 - 40\,v_7} + 0.00000000990 + 0.00000000010\,e^{40\,v_5 - 40\,v_6} = 0$
f_8	$\frac{1}{30000}\,v_8 - \frac{1}{30000}\,v_9 + 0.000000010\,e^{40\,v_8 - 40\,v_6} - 0.000000010 = 0$
f_9	$-\frac{1}{1000}\,v_1 - \frac{1}{30000}\,v_8 + \frac{31}{30000}\,v_9 + 0.00000000990\,e^{40\,v_{11} - 40\,v_{10}} + 0.00000000010 - 0.000000010\,e^{40\,v_{11} - 40\,v_9} = 0$
f_{10}	$\frac{1}{100}\,v_{10} - 0.000000010\,e^{40\,v_{11} - 40\,v_{10}} + 0.00000000990 + 0.00000000010\,e^{40\,v_{11} - 40\,v_9} = 0$
f_{11}	$\frac{1}{10000}\,v_{11} - \frac{1}{10000}\,v_{12} + 0.00000000010\,e^{40\,v_{11} - 40\,v_{10}} - 0.00000001000 + 0.00000000990\,e^{40\,v_{11} - 40\,v_9} = 0$
f_{12}	$-\frac{1}{4000}\,v_1 - \frac{1}{10000}\,v_{11} + \frac{7}{20000}\,v_{12} + 0.00000000990\,e^{40\,v_{13}} + 0.00000000010 - 0.000000010\,e^{40\,v_{13} - 40\,v_{12}} = 0$
f_{13}	$-\frac{1}{10000}\,v_1 + \frac{11}{10000}\,v_{13} + 0.00000000010\,e^{40\,v_{13}} - 0.00000001000 + 0.00000000990\,e^{40\,v_{13} - 40\,v_{12}} = 0$
f_{14}	$v_1 - 12 = 0$

TABLE III: Nodal equations

Then, the circuit is solved using double bounded Homotopy, resulting in the convergence to the 3 known solutions for the circuit. The Homotopy path that corresponds to the current for the voltage source I_E is shown in figure 11. Finally, the final point for the Homotopy trace is shown in table IV.

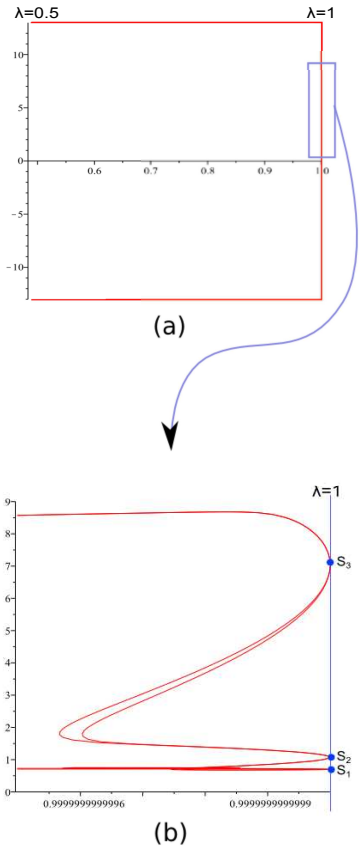

Fig. 11: Homotopy path $\lambda - v_8$

D. Chua's circuit

The following circuit [13] (see figure 12a), contains 9 solutions, has become the reference circuit for the Homotopy applied to circuit analysis. Values of the components are shown in figure VI. This circuit has 4 bipolar transistors modeled using Ebers-Moll for the bipolar transistor operating in the direct active region (see figure 12b).

The resulting equation system is:

$$
\begin{aligned}
&f_1 = 4.3663v_2 + 0.6103168 \times 10^{-5}e^{(40v_1)} - 12 \\
&+0.2863168 \times 10^{-5}e^{(40v_2)} = 0 \\
&f_2 = 5.4v_1 + v_3 + 0.3580 \times 10^{-5}e^{(40v_1)} - 22 \\
&+7 \times 10^{-7}e^{(40v_3)} + 5 \times 10^{-7}e^{(40v_4)} + 0.6620 \times 10^{-5}e^{(40v_2)} = 0 \\
&f_3 = 4.3663v_4 + 0.6103168 \times 10^{-5}e^{(40v_3)} - 12 \\
&+0.2863168 \times 10^{-5}e^{(40v_4)} = 0
\end{aligned}
\tag{18}
$$

Now, the DBH is applied to solve the circuit. The Homotopy formulation is expressed as:

$$
\begin{aligned}
H_1(f_1, \lambda) &= \lambda(\lambda - 1)(v_1 - 5)(v_1 + 5) - (\lambda - 0.5)^2 f_1^2 = 0 \\
H_2(f_2, \lambda) &= \lambda(\lambda - 1)(v_2 - 5)(v_2 + 5) - (\lambda - 0.5)^2 f_2^2 = 0 \\
H_3(f_3, \lambda) &= \lambda(\lambda - 1)(v_3 - 5)(v_3 + 5) - (\lambda - 0.5)^2 f_3^2 = 0 \\
H_4(f_4, \lambda) &= \lambda(\lambda - 1)(v_4 - 5)(v_4 + 5) - (\lambda - 0.5)^2 f_4^2 = 0
\end{aligned}
$$

where bounding lines are $a = 0$ and $b = 1$, and the initial point for the Homotopy path is selected as $A = [v_1 = -5.2, v_2 = -5.2, v_3 = -5.2, v_4 = -5.2]$.

Equilibrium equation is the same as employed in [13]. The variables to be solved are branch voltages: v_1, v_2, v_3 and v_4. Figure 13 shows the Homotopy path for branch voltage v_1. The final point for the path was $B = [v_1 = -5.2, v_2 = -5.2, v_3 = 5.2, v_4 = -5.2]$. Finally, Homotopy was able to locate all the 9 solutions in just one path. This result is interesting considering that in recent works [19][4] (applied to the same circuit) only one solution was found or some solutions were found by selecting (random or arbitrary) different initial points, that is, different and unconnected Homotopy paths.

Point	v_1	v_2	v_3	v_4	v_5	v_6	v_7	v_8	v_9	v_{10}	v_{11}	v_{12}	v_{13}	i_E
Initial $\boldsymbol{x_i}$	+13	-13	-13	-13	-13	-13	-13	-13	-13	-13	-13	-13	-13	-13
Final $\boldsymbol{x_f}$	+13	+13	-13	-13	+13	+13	+13	+13	-13	+13	-13	-13	-13	+13

TABLE IV: Initial and final point for the Homotopy path for the circuit in figure 9.

Sol	v_1	v_2	v_3	v_4	v_5	v_6	v_7	v_8	v_9	v_{10}	v_{11}	v_{12}	v_{13}	i_E
S_1	12	5.995	0.085	0.368	0.712	0.436	0.390	0.699	11.635	0.4e-5	0.039	0.039	0.321	-0.0089
S_2	12	0.883	0.278	0.590	0.631	0.812	0.315	1.074	11.647	0.4e-5	0.039	0.039	0.321	-0.0100
S_3	12	0.405	0.366	0.685	0.349	6.796	0.070	7.038	11.839	0.4e-5	0.039	0.039	0.321	-0.0085

TABLE V: Operating points (solutions) for figure 9.

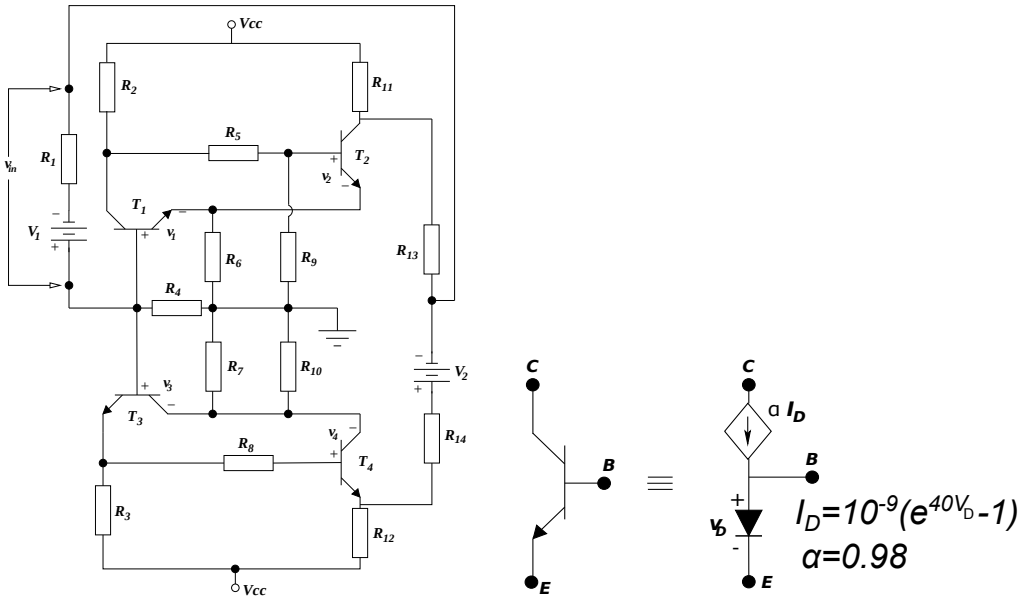

(a) Chua's circuit with 9 solutions.

(b) Half-sided Ebers-Moll model.

Fig. 12: Chua's circuit.

Component	Value	Component	Value
R_1	$1k\Omega$	R_9	$10.1k\Omega$
R_2	$4k\Omega$	R_{10}	$10.1k\Omega$
R_3	$4k\Omega$	R_{11}	$4k\Omega$
R_4	$5k\Omega$	R_{12}	$4k\Omega$
R_5	$30k\Omega$	R_{13}	$30k\Omega$
R_6	$0.5k\Omega$	R_{14}	$30k\Omega$
R_7	$0.5k\Omega$	V_1	$10V$
R_8	$30k\Omega$	V_2	$2V$
V_{CC}	$12V$	α	0.98

TABLE VI: Values of the components for the circuit shown in figure 12a.

Found solutions are:

$$\begin{bmatrix} v_1 \\ v_2 \\ v_3 \\ v_4 \end{bmatrix} = \underbrace{\begin{bmatrix} -1.0510 \\ 0.3775 \\ 0.3845 \\ -3.9542 \end{bmatrix}}_{\text{Solution } S_1}, \underbrace{\begin{bmatrix} -0.7119 \\ 0.3775 \\ 0.3350 \\ 0.3653 \end{bmatrix}}_{\text{Solution } S_2}, \underbrace{\begin{bmatrix} -0.5136 \\ 0.3775 \\ -0.9682 \\ 0.3775 \end{bmatrix}}_{\text{Solution } S_3},$$

$$\underbrace{\begin{bmatrix} 0.3242 \\ 0.3703 \\ -1.0395 \\ 0.3775 \end{bmatrix}}_{\text{Solution } S_4}, \underbrace{\begin{bmatrix} 0.3300 \\ 0.3680 \\ 0.3367 \\ 0.3642 \end{bmatrix}}_{\text{Solution } S_5}, \underbrace{\begin{bmatrix} 0.3369 \\ 0.3641 \\ 0.3836 \\ -3.7069 \end{bmatrix}}_{\text{Solution } S_6},$$

$$\underbrace{\begin{bmatrix} 0.3830 \\ -3.5446 \\ 0.3851 \\ -4.0990 \end{bmatrix}}_{\text{Solution } S_7}, \underbrace{\begin{bmatrix} 0.3857 \\ -4.2738 \\ 0.3322 \\ 0.3669 \end{bmatrix}}_{\text{Solution } S_8}, \underbrace{\begin{bmatrix} 0.3869 \\ -4.6321 \\ -0.8002 \\ 0.3775 \end{bmatrix}}_{\text{Solution } S_9}$$

V. Conclusions

A new kind of Homotopy was presented, it is named double bounded algebraic Homotopy, which contains just 2 solution lines. Also, various properties were demonstrated like the curvature radius at solutions and return points; here it was determined the influence of C and a on how acute the Homotopy path could be. Besides, it was demonstrated the symmetry of the Homotopy paths as well as the crossing point of the path through the symmetry axis. Additionally, it was illustrated the use of Homotopy in a mathematical and several circuital cases, showing its potential to be employed in analysis of non-linear circuits.

References

[1] L. O. Chua and A. Ushida, *A switching-parameter algorithm for finding multiple solutions of nonlinear resistive circuits*, International Journal of Circuit Theory and Applications **4** (1976), no. 3, 215–239.

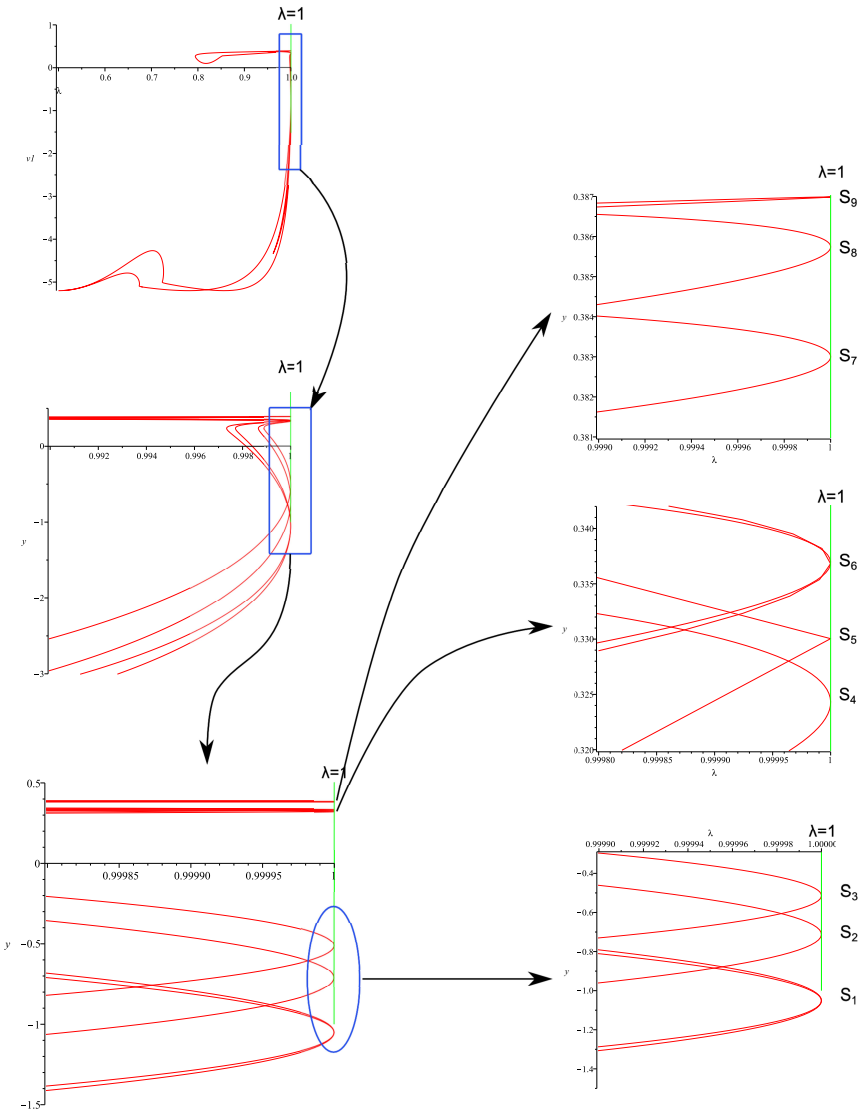

Fig. 13: Solutions for Chua's circuit.

[2] J. E. Dennis and Jorge J. Moré, *Quasi-Newton methods, motivation and theory*, Siam Review **19** (1977), no. 1.

[3] M. M. Green, *An efficient continuation method for use in globally convergent dc circuit simulation*, ISSSE Proceedings (1995), 497–500.

[4] J. Lee and C. Hsiao-D, *Constructive homotopy methods for finding all or multiple dc operating points of nonlinear circuits and systems*, IEEE Transactions on Circuits and Systems I-Fundamental Theory and Applications **48** (2001), no. 1, 51–66.

[5] R. C. Melville and L. Trajković, *Artificial parameter homotopy methods for the dc operating point problem*, IEEE transactions on computer-aided design of integrated circuits and systems **12** (1997), no. 6, 861–877.

[6] J. Ogrodzki, *Circuit simulation: methods and algorithms*, (1994).

[7] Roychowdhury and R. J. Melville, *Delivering global dc convergence for large mixed-signal circuits via homotopy/continuation methods*, IEEE Transactions on Computer-Aided Design of Integrated Circuits and Systems **25** (2006), no. 1, 66.

[8] Chung-Wen Ho Ruehli and P. A. Brennan, *The modified nodal approach to network analysis*, IEEE Transactions on Circuits and Systems **22** (1975), no. 6, 504.

[9] A. F. Schwarz, *Computer-aided design of microelectronic circuits and systems: Volume 1*, (1987), ISBN 0-12-632431-X.

[10] M. Shur, *Introduction to electronic devices*, (1996).

[11] S. M. Sze, *Semiconductor devices: Physics and technology*, (1985).

[12] M. Tadeusiewicz and K. Glowienka, *A contraction algorithm for finding all the dc solutions of piecewise-linear circuits*, J. Circuits, Syst. Comput. **4** (1994), 319–336.

[13] A. Ushida and L. O. Chua, *Tracing solution curves of nonlinear equations with sharp turning points*, Circuit Theory and Applications **12** (1984), 1–21.

[14] A. Ushida, Y. Yamagami, I. Kinouchi, Y. Nishio, and Y. Inoue, *An efficient algorithm for finding multiple dc solutions based on the spice-oriented newton homotopy method*, IEEE Transactions on Computer-Aided Design of Integrated Circuits and Systems **21** (2002), no. 3, 337–348.

[15] H. Vázquez-L., L. Hernández-M., and A. Sarmiento-R., *Numerical path following for double bounded homotopy scheme for analysing nonlinear resistive circuits*, IBERCHIP (2003).

[16] _____, *Double-bounded homotopy for analysing nonlinear resistive circuits*, International Symposium on Circuits

and Systems (2005).

[17] D. M. Wolf and S. R. Sanders, *Multiparameter homotopy methods for finding dc operating points of nonlinear circuits*, IEEE transactions on circuits and systems-I: fundamental theory and aplications **43** (1996), no. 10, 824–837.

[18] K. Yamamura and T. Ohshima, *Finding all solutions of piecewise-linear resistive circuits using linear programming*, IEEE transactions on circuits and systems-I: fundamental theory and aplications **45** (1998), 434–445.

[19] K. Yamamura, T. Sekiguchi, and Y. Inuoe, *A fixed-point homotopy method for solving modified nodal equations*, IEEE transactions on circuits and systems-I: fundamental theory and aplications **46** (1999), no. 6, 654–664.